JOURNAL OF THE MECHANICAL BEHAVIOR OF BIOMEDICAL MATERIALS 65 (2017) 317–333

Available online at www.sciencedirect.com

ScienceDirect

www.elsevier.com/locate/jmbbm

Research Paper

Development and characterization of cross-linked gellan gum and retrograded starch blend hydrogels for drug delivery applications

Valéria Maria de Oliveira Cardoso[a], *Beatriz Stringhetti Ferreira Cury*[b,*], *Raul Cesar Evangelista*[b,1], *Maria Palmira Daflon Gremião*[b]

[a]*Graduate Program in Pharmaceutical Sciences, Faculty of Pharmaceutical Sciences, São Paulo State University-UNESP, km 1 Araraquara-Jaú Road, Araraquara, SP, Brazil*

[b]*Department of Drugs and Pharmaceuticals, Faculty of Pharmaceutical Sciences, São Paulo State University-UNESP, km 1 Araraquara-Jaú Road, Araraquara, SP, Brazil*

ARTICLE INFO

Article history:
Received 8 March 2016
Received in revised form
19 July 2016
Accepted 1 August 2016
Available online 20 August 2016

Keywords:
Gellan gum
Retrograded starch
Hydrogels
Rheology
Structure
Texture

ABSTRACT

The retrogradation of high amylose starch (5% or 10%), by isothermal cycles at 4 °C (method 1) or by alternating thermal cycles (method 2) was efficient and promoted important structural modifications. Hydrogels of gellan gum and starch retrograded blends, containing or not ketoprofen, were prepared by ionic and dual cross-linking, at different concentrations of polymer and cross-linkers, and characterized by texture and rheological analysis, X-ray diffraction and morphological analysis. The ionic cross-linking and starch retrograded by method 1 contributed to the improvement of hardness and cohesiveness of hydrogels while the dual cross-linking and starch retrograded by method 2 favored the adhesiveness. The rising of polymer concentration lead to the improvement of all mechanical parameters. Rheological data demonstrated that non-cross-linked dispersions showed a behavior of weak gels and the cross-linked hydrogels presented a predominantly elastic behavior ($G' \gg G''$), peculiar of strong gels. X-ray diffraction, rheological data and the scanning electron microscopy (FEG-SEM) revealed that the increase of polymers and cross-linkers concentration and the presence of drug resulted in stronger and more stable tridimensional structures. The suitable adhesiveness and high strength and elasticity of hydrogels H253IC-KT, H255IC-KT, H21053DC-KT and H21055DC-KT make them more promising materials for the design of mucoadhesive drug delivery systems.

*Corresponding author. Fax: +55 16 33016960.
E-mail address: curybsf@fcfar.unesp.br (B.o.s. Stringhetti Ferreira Cury).
[1]In memoriam.

http://dx.doi.org/10.1016/j.jmbbm.2016.08.005
1751-6161/

1. Introduction

Development of innovative materials that promote effective control of drug release according to specific therapeutic needs is an exciting area of pharmaceutical research. The use of bioadhesive natural polysaccharides to achieve the spatial and/or temporal control of drug release is of great interest because of the atoxicity, low cost, high bioavailability, biodegradability of polysaccharides, and due of the fact that are easily obtained from renewable sources (Alvarez-Lorenzo et al., 2013; Bhardwaj et al., 2000; Kulkarni et al., 2011; Sinha and Kumria, 2001). However, natural polysaccharides can present some disadvantages related to their viscosity, swelling, solubility, and stability. Through the blending of polymers or their modification by cross-linking reactions, new materials can be developed with modulated physicochemical properties tailored to the specific requirements of a given application (Bajpai et al., 2008; Carbinatto et al., 2012; Carbinatto et al., 2014; Cury et al., 2009a, 2009b; Meneguin et al., 2014; Oliveira et al., 2010; Peppas et al., 2000; Prezotti et al., 2014, 2012; Soares et al., 2013).

The combination of natural polysaccharides, as well as the modification of polymers by ionic and ionic/covalent cross-linking, allows the formation of tridimensional structures consisting of macromolecular chains interconnected by covalent bonds and/or physical interactions. Such structures, also called hydrogels, are highly hydrophilic and thus able to absorb high volumes of water or biological fluids (Dragan, 2014; Hoffman, 2002; Peppas et al., 2000). Furthermore, hydrogels can efficiently entrap drugs in interstitial spaces among polymer chains by dispersion or dissolution, thereby protecting therapeutic agents from undesirable conditions in the biological environment and enabling site-specific delivery (Hennink and van Nostrum, 2012; Hoffman, 2002). Thus, polymeric hydrogels are considered very promising carriers of bioactive molecules, including proteins and peptides. Because hydrogels can be degraded in specific portions of the gastrointestinal (GI) tract, they are ideally suited for controlled drug delivery (Dragan, 2014; Hennink and van Nostrum, 2012; Hoffman, 2002; Peppas et al., 2000).

Native starch, classified as a semi-crystalline homopolysaccharide consisting of amylose and amylopectin chains, is widely used in the food and pharmaceutical industries, because it can act as a thickener, colloid stabilizer, gelling agent, and adhesive to improve food texture (Denardin and Silva, 2009; Dona et al., 2010; Kulkarni et al., 2011; Paraginski et al., 2014; Singh et al., 2003). However, the enzymatic, chemical, or physical modification of native starch is often necessary in order to modulate its properties for specific uses (Carbinatto et al., 2012; Carbinatto et al., 2014; Cury et al., 2009a, 2009b; Meneguin et al., 2014; Oliveira et al., 2010; Prezotti et al., 2014, 2012; Rioux et al., 2002; Zavareze and Dias, 2011).

The physical modification of starch by retrogradation represents a promising strategy to reach high levels of type 3 resis tant starch. The thermal stability, low solubility, and specific degradability of type 3 resistant starch by colon microbiota make it a suitable material for the design of colon-specific delivery systems (Chung et al., 2006; Haralampu, 2000; Htoon et al., 2010; Meneguin et al., 2014; Thompson, 2000).

The retrogradation of starch is performed by hydrothermal treatment in which the starch granules gelatinize and rupture, causing amylose to leach out of the granules as coiled structures. After cooling and storage, the molecules are recrystallized through several interactions including hydrogen bonds and van der Waals forces (Dona et al., 2010; Haralampu, 2000; Liu et al., 2007; Zhang et al., 2011). This slow and continuous recrystallization favors the formation of a structure with a high degree of organization and crystallinity (Hou et al., 2012; Park et al., 2009; Silverio et al., 2000).

High amylose starch (HAS) (Hylon VII®) is a modified starch, characterized by high amounts of amylose (68%). HAS is ideally suited to achieve high levels of type 3 resistant starch because the crystallites built in the retrogradation process are embedded in an amorphous matrix that protects them from exposure to enzymes (Dimantov et al., 2004a, 2004b; Htoon et al., 2009; Meneguin et al., 2014).

Gellan gum (Gelrite® or Kelcogel®) is a linear hydrophilic anionic exopolysaccharide produced as result of aerobic fermentation by *Sphingomonas elodea* (Giavasis et al., 2000) that has been widely used in food, cosmetics, toiletries and pharmaceuticals as a emulsifying, suspending, stabilizing, gelling or thickening agent, film-forming properties (Hasheminya and Dehghannya, 2013; Morris et al., 2012). Due to its anionic features, this polymer has important mucoadhesive properties (Lee et al., 2000; Narkar et al., 2010; Salamat-Miller et al., 2005). Additionally, GG has the ability to form strong gels in the presence of divalent cations, particularly Ca^{2+}, resulting in microparticles with hydrophilic tridimensional polymeric networks able to absorb high volumes of water or biological fluids (Agnihotri et al., 2006; Babu et al., 2010; Narkar et al., 2010; Patil et al., 2006; Rajinikanth and Mishra, 2007).

Polymer cross-linking is a rational approach that allow to prepare hydrogels by introducing intra and/or intermolecular bonds (Keawchaoon and Yoksan, 2011; Patil et al., 2010), resulting in three-dimensional structures with modulated properties, such as rheology (Carbinatto et al., 2012; Soares et al., 2013) and swelling (Bigi et al., 2001; Cury et al., 2009b; Prezotti et al., 2014). Furthermore, recent studies have shown that these mechanical properties can still contribute to the release modulation of different drugs like ketoprofen (Boni et al., 2015; Prezotti et al., 2014); sodium diclofenac (Cury et al., 2009a , 2009b; Soares et al., 2013), nimesulide (Carbinatto et al., 2012, 2014), glipizide (Maiti et al., 2011) and polymers proteins (Martinez et al., 2014).

In a study with carboxymethyl guar, Reddy and Tammishetti (2002) demonstrated that Al^{3+} ions promote faster cross-linking of hydrogels and that they sustain the release of bovine serum albumin. Recently, Maiti et al. (2011), demonstrated that GG microcapsules cross-linked with Al^{3+} ions displayed an increased glipizide release time, because each ion was able to establish multiple linkages with the carboxyl groups of the gellan chains, resulting in a stronger gel structure. Prezotti et al. (2014) also reported that microspheres of GG/pectin blends (cross-linked with Al^{3+}) allowed

the effective control of drug release rates in acid media (pH 1.2) and phosphate buffer (pH 6.0).

Dual cross-linking (DC) has been used as a strategy to adjust the mechanical properties of materials according to their intended uses, allowing for more effective control of drug release rates (Hou et al., 2012; Kulkarni et al., 2011; Ofokansi et al., 2013; Phromsopha and Baimark, 2014). In a study with gelatin and albumin microparticles, Kulkarni et al. (2011) reported that the reaction with Ca^{2+} ions and glutaraldehyde, respectively, through dual cross-linking, resulted in a more effective control of drug release rates than those promoted only by ionic cross-linking (IC).

In recent years, several researches have reported that drug delivery systems based on polymeric hydrogels has allowed the effective temporal and/or spatial control of drug release rates (Calixto et al., 2015; Carvalho et al., 2013; Chaturvedi et al., 2013; Contri et al., 2014; Gao et al., 2016; Maulvi et al., 2016). In this sense, the exploitation of blends of the natural polysaccharides gellan gum and retrograded starch modified by ionic or dual cross-linking is a rational approach to reach new materials with specific properties that can attend to different uses as the design of innovative mucoadhesive drug delivery systems.

As such, the modulation of structural and mechanical properties of hydrogels allows the optimization of drug delivery systems, improving therapeutic responses. The aim of this work was to evaluate the influence of the starch retrogradation method, the polymers concentration, and the cross-linking process on the mechanical and structural properties of hydrogels of GG/retrograded starch blends, evaluating their potential for controlled drug delivery applications.

2. Materials and methods

2.1. Materials

High amylose starch (HAS) (Hylon VII – 68% amylose, lot: HA9140) was a gift from National Starch & Chemical (New Jersey, EUA). Gellan gum (GG) (type Kelcogel® CG-LA) was kindly provided by CP Kelco (Limeira, SP, Brazil). The following materials were commercially obtained: ketoprofen (KT) (batch #9072223; Zhejiang Jiuzhou Pharmaceutical Co., Taizhou, China) used as model drug, aluminum chloride (Duque de Caxias, Brazil), glutaraldehyde (Sigma Aldrich®, St. Louis, MO, USA), and purified water (Milli Q, Millipore) (Molsheim, France).

2.2. Retrogradation of high amylose starch (HAS)

HAS was retrograded based on a previously reported method (Park et al., 2009). Briefly, aqueous dispersions of HAS (5% or 10% m/v) were prepared under mechanical stirring during 30 min. These dispersions were autoclaved (121 °C/1 atm, 15 min) to pre-gelatinize the HAS and subsequently cooled at room temperature. The gelatinized HAS was subjected to two different methods of retrogradation. Method 1 (M1) consisted of isothermal cooling (4 °C) during 8 days, while method 2 (M2) involved alternating temperature cycles (4 °C and 30 °C, 2 days in each temperature) during 16 days. The retrograded starch (RS) dispersions obtained by the two methods were named RS-M1 and RS-M2.

2.3. Preparation of polymeric dispersions

2.3.1. GG/RS-M1 and GG/RS-M2 dispersions

Aqueous dispersions of GG (1% or 2%, m/v) were prepared in previously heated purified water (80 °C) and kept under mechanical stirring for 20 min, at room temperature. Retrograded starch (RS-M1 or RS-M2) gels (5% or 10%, m/v), prepared as item 2.2, were kept under mechanical stirring (20 min) at room temperature for complete homogenization. Then, RS dispersions were added to GG dispersions (1:1 v/v), and kept under mechanical stirring at room temperature for 20 min.

For dispersions containing KT, the drug was incorporated (0.5%, m/v) after mixing the RS and GG dispersions, while the blend was kept under mechanical stirring, at room temperature. These dispersions were labeled according to the polymer concentration, using the D prefix (dispersions) and KT suffix when containing KT. For example D210 is a dispersion containing 2% of gellan gum and 10% of retrograded starch. The label of all dipersions are described in Table 1.

2.3.2. Ionically cross-linked (IC) hydrogel preparation

Aluminum chloride (Al^{3+}) (3% or 5% of dry polymer mass) was added to the dispersions (obtained as discussed in 2.3.1) under mechanical stirring for 20 min at room temperature.

2.3.3. Dual cross-linked (DC) hydrogels preparation

Glutaraldehyde (1%, 3% or 5% of dry polymer mass) was added to the IC hydrogels (obtained as discussed in 2.3.2) under mechanical stirring for additional 20 min at room temperature.

Cross-linked hydrogels were labeled according to the concentration of polymers (GG and RS) and cross-linker (Al^{3+} and glutaraldehyde). H prefixes were added for hydrogels, and IC or DC suffixes for ionic cross-linking and dual cross-linking, respectively. For example, H21053DC represents a dual cross-linked hydrogel prepared with gellan gum 2%, retrograded starch 10%; aluminum chloride 5% and glutaraldehyde 3%, while H1103IC is related to the ionically crosslinked hydrogel prepared with gellan gum 1%, retrograded starch 10% and aluminum chloride 3%. The label of all samples are described in Table 1.

2.3.4. Ionically cross-linked and dual cross-linked GG gels preparation

Ionically cross-linked (GG-IC) and dual cross-linked (GG-DC) GG gels (Table 2) were prepared for comparative texture profile analysis (TPA). Aqueous dispersions of GG (1% or 2%) in purified water at 80 °C were prepared under mechanical stirring for 20 min, and then cross-linker solutions were added following the procedure previously described for IC and DC hydrogels (2.3.2 and 2.3.3), respectively.

The texture properties of RS-M1 and RS-M2 gels could not be measured due to their low viscosity.

Table 1 – Composition of ionically and dually cross-linked GG/RS hydrogels and selected samples for rheological analysis (#ce:cross-ref id="cr0005" refid="tbl1fnStar"##ce:sup##ce:bold#⁎#/ce:bold##/ce:sup##/ce:cross-ref>).

Samples	Gellan (%)	RS (%)	Cross-linkers (%)		Nomenclature
			Al^{3+}	Glu	
IC	1	5	3	–	H153IC*
			5	–	H155IC
		10	3	–	H1103IC*
			5	–	H1105IC
	2	5	3	–	H253IC*
			5	–	H255IC*
		10	3	–	H2103IC*
			5	–	H2105IC*
DC	1	5	3	1	H1531DC
				3	H1533DC
				5	H1535DC*
			5	1	H1551DC
				3	H1553DC*
				5	H1555DC
		10	3	1	H11031DC
				3	H11033DC
				5	H11035DC
			5	1	H11051DC
				3	H11053DC
				5	H11055DC
	2	5	3	1	H2531DC
				3	H2533DC
				5	H2535DC
			5	1	H2551DC
				3	H2553DC*
				5	H2555DC
		10	3	1	H21031DC*
				3	H21033DC*
				5	H21035DC*
			5	1	H21051DC*
				3	H21053DC*
				5	H21055DC*

* Selected samples for rheological analysis.

2.4. Texture profile analysis (TPA)

The texture properties of polymeric hydrogels (Table 1) were analyzed on a TA-XT2 Texture Analyzer (Stable Micro Systems) (Godalming, United Kingdom) operating in TPA mode. Each sample (10 g) was introduced in a Falcon 50 mL conical tubes (16 mm × 100 mm) and compressed twice ($v = 0.50$ mm s^{-1}; depth 10 mm) by the cylindrical analytical probe (10 mm diameter), allowing a relaxation time of 5 s between the compressions. Force *versus* time curves were generated by Texture Exponent Lite software during two cycles of compression, and the hardness, cohesiveness, and adhesiveness were determined. The analysis was performed at room temperature for 5 independent replicates.

Once the equipment has no heating system, the analysis were performed at room temperature, verifying the possibility to take the test under these conditions according to other published studies (Calixto et al., 2015; Calixto et al., 2016; Carvalho et al., 2013).

Table 2 – Composition of ionically and dually cross-linked gellan gels.

Group	Gellan (%)	Cross-linkers (%)		Nomenclature
		Al^{3+}	Glu	
IC-GG	1	3	–	GG13IC
		5	–	GG15IC
	2	3	–	GG23IC
		5	–	GG25IC
DC-GG	1	3	1	GG131DC
			3	GG133DC
			5	GG135DC
		5	1	GG151DC
			3	GG153DC
			5	GG155DC
	2	3	1	GG231DC
			3	GG233DC
			5	GG235DC
		5	1	GG251DC
			3	GG253DC
			5	GG255DC

2.5. Viscoelastic property analysis

The viscoelastic properties of selected samples (Table 1), containing or not KT, were determined on a rotational rheometer (Advanced Rheometer AR2000ex, TA instruments Ltd) using Rheology Advantage Data Analysis software (version 5.7.1 V) for data acquisition. The analyses were performed using the parallel-plates geometry set (40mm diameter, 1mm gap) at 37 °C. Before each measurement, the samples were allowed to stand for 1 min. Stress sweeps were recorded between 0.1 and 100 Pa at constant frequency (1 Hz) to determine the linear viscoelastic region. Mechanical spectra were obtained at constant stress (5 Pa) under an angular velocity range of 0.6–623 rad s^{-1}. Non-cross-linked GG/RS dispersions (2.3.1) were also analyzed for comparison. The tests were conducted in triplicate.

2.6. Morphology of hydrogels

The morphology of non-cross-linked dispersion and of IC and DC hydrogels (Table 4) was analyzed by field emission gun scanning electron microscopy (FEG-SEM) (JEOL JSM-7500F, Japan). The dispersions and IC and DC hydrogels, containing or not KT, were prepared as described in item 2.3.1, 2.3.2 and 2.3.3, respectively, and immediately frozen with liquid nitrogen and then lyophilized for 24 h. The lyophilized samples were fractured and were attached in the sample holder with a double-side adhesive tape and photomicrographs at various magnifications were taken.

2.7. X-ray diffraction (XRD) analysis

Crystallinity patterns of KT, isolated polymers (HAS, RS (5% and 10%) and GG (1% and 2%)), lyophilized GG/RS dispersions and lyophilized IC and DC GG/RS blends hydrogels (Table 4) were evaluated from their diffractograms resulting from

Table 3 – G′ (stress, 1 Pa and frequency, 1 Hz), linear regression (*r*), viscoelastic exponent (*n*), and gel strength (*S*) of the uncross-linked dispersions, ionically and dually cross-linked GG/RS hydrogels, containing or not ketoprofen.

Samples	G′	n′	r	n	S
D15	0.12	0.08	0.17	23.77	0.00
D15-KT	0.52	0.11	0.42	1.39	0.03
D110	8.14	2.55	0.06	55.17	0.00
D110-KT	39.18	1.89	0.07	0.33	17.65
D25	38.78	1.92	0.43	0.71	2.99
D25-KT	179.77	6.49	0.80	0.43	47.07
D210	147.20	6.40	0.70	0.38	51.37
D210-KT	393.50	13.11	0.38	0.22	244.19
H153IC	1290.03	32.07	0.95	0.14	962.69
H153IC-KT	1780.67	44.43	0.96	0.14	1304.36
H253IC	5828.00	145.67	0.99	0.10	1471.93
H253IC-KT	8660.00	217.33	0.99	0.11	2366.60
H255IC	6202.67	163.13	0.98	0.11	4638.28
H255IC-KT	9159.33	235.20	0.99	0.11	6846.63
H1103IC	1830.00	43.28	0.99	0.12	4807.95
H1103IC-KT	3012.33	71.59	0.98	0.12	7171.01
H2103IC	7894.67	192.07	0.99	0.11	6226.73
H2103IC-KT	7854.33	192.67	0.99	0.12	5869.76
H2105IC	7612.67	189.73	0.99	0.12	5956.48
H2105IC-KT	6656.33	162.13	0.99	0.11	5320.60
H1535DC	853.63	19.71	0.89	0.16	596.52
H1535DC-KT	1895.33	46.24	0.97	0.12	1472.58
H1553DC	1562.33	38.01	0.92	0.16	1103.92
H1553DC-KT	809.87	20.25	0.83	0.15	589.38
H2553DC	9539.67	250.73	0.99	0.12	7422.28
H2553DC-KT	3980.67	101.79	0.99	0.12	3073.95
H21031DC	6770.67	168.13	0.99	0.11	5335.83
H21031DC-KT	5400.00	137.70	0.99	0.12	4227.00
H21033DC	6485.67	183.20	0.98	0.13	4998.57
H21033DC-KT	8866.00	208.97	0.99	0.11	6982.18
H21035DC	6283.00	123.47	0.99	0.11	4959.58
H21035DC-KT	8431.33	196.97	0.99	0.11	6674.79
H21051DC	7478.67	191.63	0.99	0.11	5880.32
H21051DC-KT	5973.00	142.35	0.99	0.11	4739.12
H21053DC	6033.33	145.13	0.99	0.11	4795.90
H21053DC-KT	10726.00	254.20	0.99	0.11	8592.95
H21055DC	5845.67	141.90	0.99	0.12	4565.62
H21055DC-KT	10690.00	251.23	0.99	0.11	8528.99

analysis X-ray diffractometer (Siemens® – Model D5000; Germany), using nickel-filtered Cu Kα radiation (λ=1.5406 A°) (tube operating at 40 kV and 30 mA). The scanning regions were collected from 4° to 50° (2θ) in step size of 0.05° (2θ).

2.8. Statistical analysis

In texture profile and viscoelastic property analysis, the results were treated by one-way analysis of variance (ANOVA) followed by Tukey test to evaluate significant differences (Origin 7.0 software). In these tests, values of $p<0.05$ were considered statistically significant.

3. Results and discussion

3.1. Starch retrogradation

The improvement of functional and structural properties of starch can be determined by the changes that it undergoes during retrogradation process (pre-gelatinization and storage). This changes involve water uptake, granule break, swelling and formation of a viscous paste (gelatinization) followed by recrystallization of starch chains (retrogradation) (BeMiller, 2011; Wang et al., 2015). In this work, starch retrogradation was performed based on a previously reported method (Park et al., 2009), in which, after the hydrothermal treatment (121 °C/1 atm, 15 min), the pre-gelatinized HAS was subjected to two different methods of retrogradation: isothermal cooling (4 °C) during 8 days (RS-M1) and alternating temperature cycles (4 °C and 30 °C, 2 days in each temperature) during 16 days (RS-M2).

Starch retrogradation mechanism occurs by thermoreversible recrystallization which is based in three stages called nucleation (the formation of crystals critical core), propagation (crystals core growth) and maturation (crystal growth and/or perfection). The starch retrogradation degree and extent depends of the propagation and nucleation rate of the crystals formed, and can be affected mainly by storage conditions, such as temperature and time. Temperature near

Table 4 – Non-cross-linked dispersions, ionically and dually cross-linked GG/RS hydrogels, containing or not ketoprofen, selected by rheological assay, to analysis in FEG-SEM and X-ray diffraction patterns.

Samples	Gelan (%)	RS (%)	Cross-linkers (%)		Nomenclature	
			Al^{3+}	Glu	Without KT	With KT
Dispersions	1	5	–	–	D15	D15-KT
			–	–	D25	D25-KT
	2	10	–	–	D210	D210-KT
IC	1	5	3	–	H153IC	H153IC-KT
	2	5		–	H253IC	H253IC-KT
			5	–	H255IC	H255IC-KT
DC	1	5	3	5	H1535DC	H1535DC-KT
	2	5	5	3	H2553DC	H2553DC-KT
		10	3	1	H21031DC	H21031DC-KT
			5		H21051DC	H21051DC-KT
				3	H21053DC	H21053DC-KT
				5	H21055DC	H21055DC-KT

of the Tg (glass transition temperature) (~6 °C) favors the nucleation, while temperature around 30 °C favors propagation (Park et al., 2009; Silverio et al., 2000; Zhou et al., 2010).

In this sense, during the storage under cooled conditions (4 °C/8 days), the nucleation process is favored by the fast recrystallization, in which the large amount of small-size crystallites are formed and homogeneously dispersed among the amylose and amylopectin chains.

Recent studies reported that retrogradation is a continuous process promoted by rapid recrystallization of amylose followed by a slow recrystallization of amylopectin (Li et al., 2016; Wang et al., 2015; Yu et al., 2009). In this sense, in isothermal retrogradation under cooling conditions, initially a fast recrystallization of amylose should occur and with the increasing of storage time (until 8 days), a long-term recrystallization of the amylopectin molecule is expected, making the network continuously more organized and thermodynamically stable.

On the other hand, the retrograded starch under cycled temperature (4 ° C and 30 °C/16 days) must have a looser and stable structural network constituted of perfects crystallites distributed homogeneously over network. This behavior is coherent, because in a study about the retrogradation of waxy starch, Park et al. (2009) based on DSC analysis concluded that in alternating cycles (4 ° C and 30 °C/ 16 days), more imperfect crystals can melt at 30 °C, reaching a new and more ordered structure according the storage time (until 16 days), so that in the final of the retrogradation process, more perfect and stable crystals are built.

3.2. *Analysis of the mechanical properties of polymeric hydrogels*

The hardness of solid materials expresses its resistance against deformation, i.e., the maximum force required for deformation of the sample (Jones et al., 1997). For IC hydrogels, in general, higher hardness values were obtained for samples with higher GG concentrations (2%), containing RS-M1 (5% and 10%) ($p<0.05$). These values were also higher than those of GG-IC ($p<0.05$). The highest hardness value was observed for the sample H2105IC ($p<0.05$) (Fig. 1A).

The increased concentration of both polymers in the hydrogel leads to the formation of a more packed network, caused by high levels of interpenetration and entanglement of polymer chains. Rodríguez-Hernandes et al. (2006), in studies about the structural properties of blends of unmodified waxy maize starch granules and GG reported the formation of more compact networks when starch was present. Huang et al. (2007) demonstrated that the high concentrations of the rice starch and GG improved the hardness of the hydrogels.

Additionally, our results demonstrate that in the ionic cross-linking, the presence of cations can decrease the repulsion of anionic polymeric chains by increasing the amount of intra and/or interchain junction zones (Bajpai et al., 2008; Oliveira et al., 2010; Prezotti et al., 2014; Souto-Maior et al., 2010). This allows the building of a more dense and compact network, contributing to the higher hardness of IC hydrogels.

The greater hardness values of hydrogels containing RS-M1 in comparison to those containing RS-M2 (Fig. 1A) indicate that the recrystallization of amylose, which occurs in shorter time (Li et al., 2016; Yu et al., 2009; Wang et al., 2015) favored the hardness of the hydrogels prepared in this work. The building of more rigid structures due to the continuous

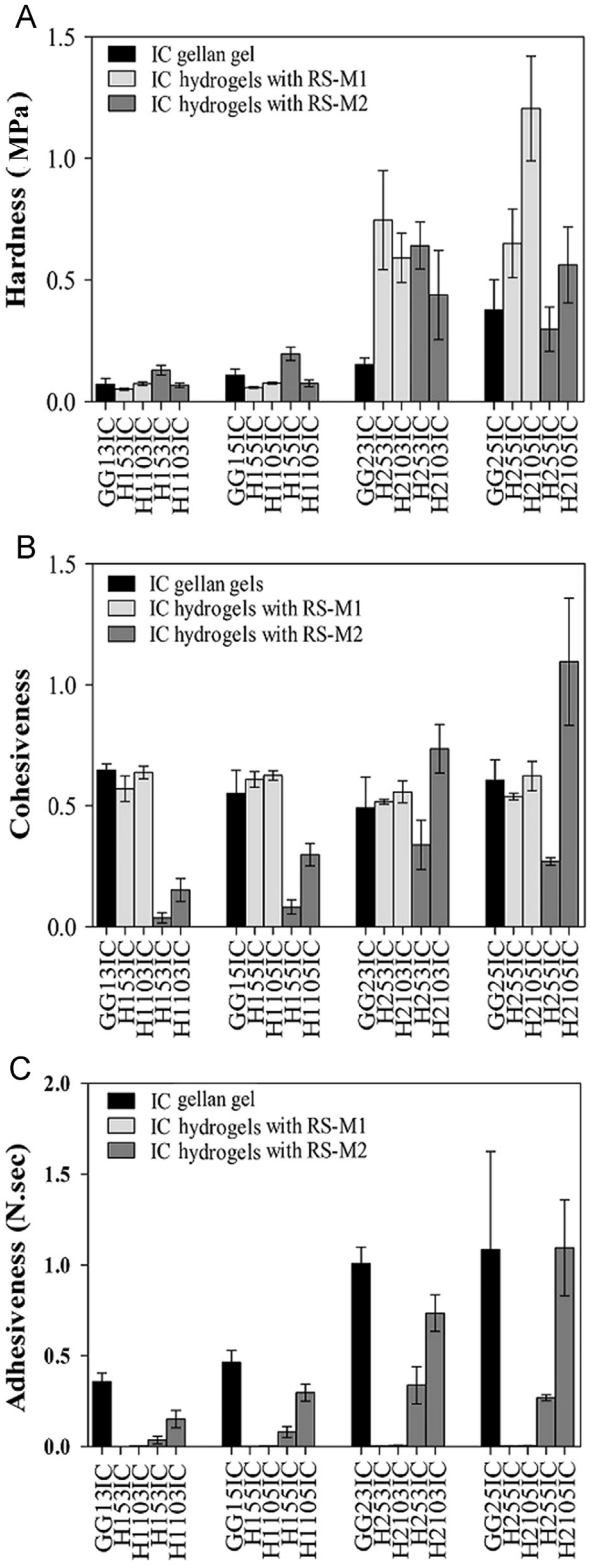

Fig. 1 – Mechanical properties of ionically cross-linked GG/RS and GG hydrogels: (A) Hardness, (B) cohesiveness, and (C) adhesiveness.

organization of polymer network during isothermal cooling (4 and 30° C/16 days) was previously reported by Park et al. (2009).

For DC hydrogels (Fig. 2), in general, the highest hardness values were obtained for hydrogels containing RS-M1 and maximum concentrations of both polymers ($p<0.05$), independent of the cross-linker concentration (Fig. 2A). The hardness values of the DC hydrogels were higher than those of GG-DC ($p<0.05$) and the highest hardness values were exhibited by the samples H21053DC and H21055DC ($p<0.05$) (Fig. 2A).

In a comparative analysis between IC and DC hydrogels, the highest hardness values were reached by IC hydrogels containing RS-M1 ($p<0.05$). This observation can be attributed to the excessive rigidity of networks built by dual cross-linking. Due to the introduction of covalent bonds, these structures are more brittle and the hydrogels are more easily broken when stress is applied. Instead, IC allowed the formation of a looser network resulting in hydrogels that support higher levels of stress.

Cohesiveness expresses the internal structure ability of a material maintain itself strongly interconnected with certain

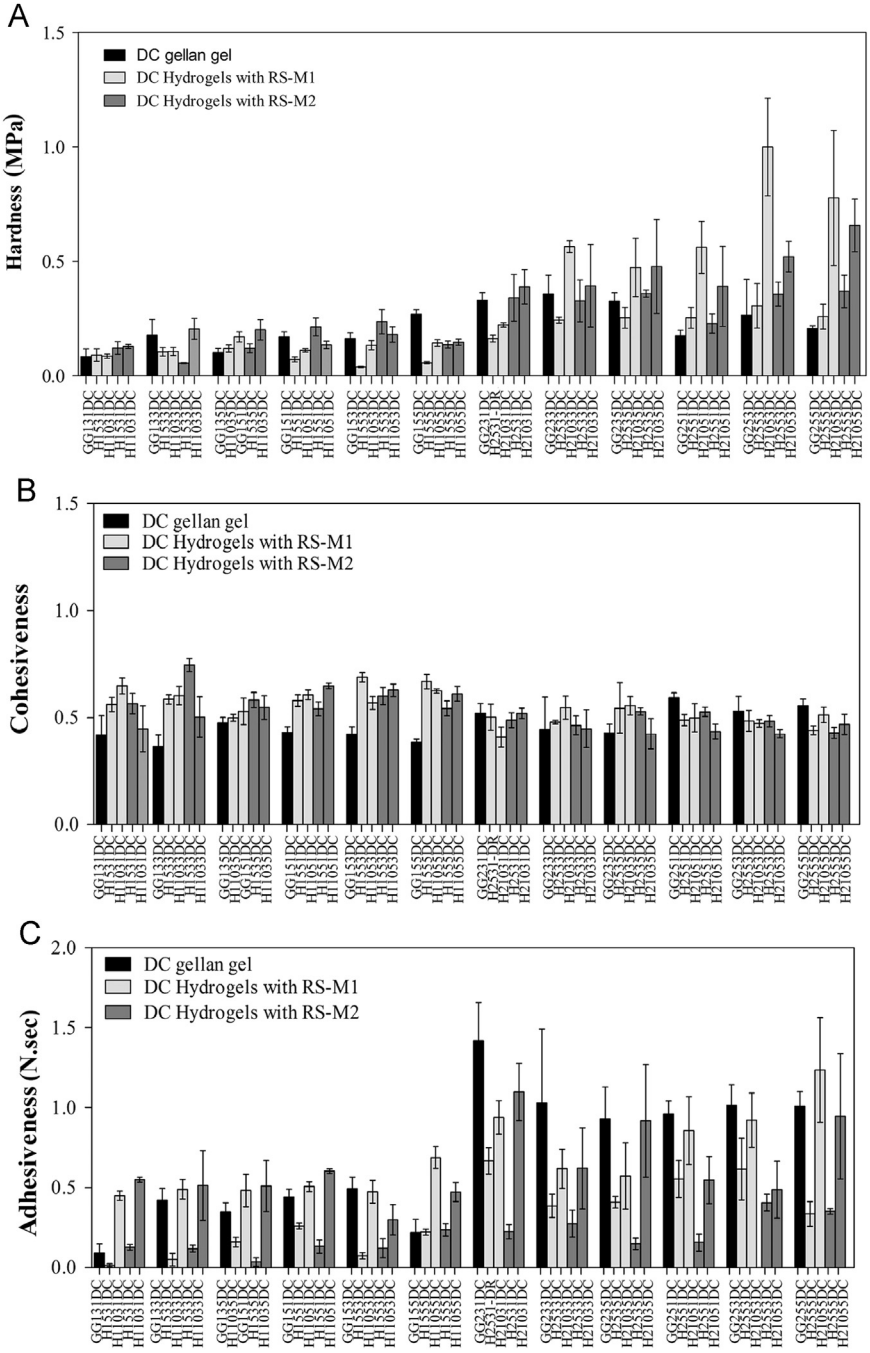

Fig. 2 – Mechanical properties of dually cross-linked GG/RS and GG hydrogels: (A) Hardness, (B) cohesiveness, and (C) adhesiveness.

level of resistance against rupture (Lau et al., 2000; Morris et al., 2012). Cohesiveness values showed no significant difference among the IC hydrogels containing RS-M1 ($p>0.05$), independent of polymer and cross-linker concentrations. The same behavior was observed in relation to GG-IC ($p>0.05$). However, the cohesiveness of hydrogels containing RS-M1 was higher than that of hydrogels with RS-M2 ($p<0.05$) (Fig. 1B). Considering that the temperature of 4 °C favor the nucleation, it is possible that a great number of small crystallites can be built, which can be arranged in interchains spaces, acting as a physical cross-linking, resulting in a more packed and cohesive structure.

Among the hydrogels prepared with RS-M2, the highest cohesiveness values were achieved when both polymers were at their maximum concentration (H2103IC and H2105IC) ($p<0.05$) (Fig. 1B). Again, the results show that blending of polymers and increasing their concentration contributes to the formation of more entangled networks.

For DC hydrogels, in general, it was observed that the cohesiveness values did not show statistically significant differences between all samples ($p>0.05$) (Fig. 2B).

Although the cohesiveness of the IC and DC hydrogels containing RS-M1 did not exhibit statistically significant differences for each group ($p>0.05$), in the hydrogels containing RS-M2, the cohesiveness of IC hydrogels was higher than that of DC hydrogels when the highest concentrations of both polymers was used ($p<0.05$) (H2103IC and H2105IC), independent of the cross-linker concentration. Probably in these conditions, with high concentration of polymers more contact points intra- and inter-chains were established, creating entanglement and/or junction zones between polymeric chains, resulting in a strong and cohesive network.

Adhesiveness expresses the ability of a material to adhere to a given material, i.e., the total force required to separate the probe of the sample (Huang et al., 2007). Both IC hydrogels, containing RS-M1 and RS-M2, presented adhesiveness lower than GG-IC ($p<0.05$), except for H2105IC with RS-M2, which showed similar adhesion levels to GG25IC (Fig. 1C).

Among samples containing RS-M1, in general, it was observed that the adhesiveness values did not show statistically significant differences between all samples ($p>0.05$) (Fig. 1C). However, IC hydrogels containing RS-M2 showed higher adhesiveness values when both polymers (GG and RS-M2) were at maximum concentration, being the highest adhesiveness exhibited by hydrogel H2105IC ($p<0.05$).

For DC hydrogels, adhesiveness was higher in samples with RS-M1 (Fig. 2C), and the H21055DC sample exhibited the highest adhesiveness value ($p<0.05$). In relation to the GG-DC, DC hydrogels showed lower adhesiveness in general ($p<0.05$).

In a comparative analysis between IC and DC hydrogels, the highest adhesiveness was observed for DC hydrogels containing RS-M2 ($p<0.05$) (Fig. 2C).

The set of results demonstrated that, in general, IC contributed to increased hardness and cohesiveness of hydrogels, while DC increased adhesiveness of these materials. High concentrations of both polymers positively affected all three parameters.

In this study, the adhesiveness was considered a fundamental property because it is a promising ability for further preparation of mucoadhesive drug delivery systems. Thus, the samples containing RS-M2 were selected for the further assays because this material improved the adhesiveness of hydrogels. On the other hand, hardness and cohesiveness are parameters that should influence the physical stability of hydrogels in the biological medium. In this sense, samples with low, intermediate and high degrees of adhesiveness, hardness and cohesiveness were selected for further studies (Table 1).

3.3. *Rheological properties of polymeric hydrogels*

Rheological analysis is often used to characterize systems that consist of one or more polymeric material and that present changes in their mechanical strength after cross-linking (Berger et al., 2004; Kulkarni et al., 2011), and consequently in their elasticity behavior (Grassi et al., 2006; Khondkar et al., 2007; Romani et al., 2002). In polymeric materials, the viscoelastic behavior is due to highly cross-linked domains (apparent elastic domains) in the polymer structure, while the fluid character is attributed to non-cross-linked domains (apparently viscous domains) (Grattoni et al., 2001).

The use of rheological tests for the characterization of hydrogels provides important information about their viscoelastic properties and helps to establish a correlation between the internal structure of a hydrogel and its rheological behavior (Dinu et al., 2012).

By analysis of stress sweep spectra of all samples (cross-linked and non-cross-linked) (Fig. 3), it was found that for non-cross-linked dispersions (Fig. 3A) the linear viscoelastic range presented in the lower regions (about 1 Pa), indicating that this structures are weaker and easily broken at low stress. These samples exhibited the smallest critical stress values, demonstrating disruption of the system structure close to 1 Pa. Therefore, for the cross-linked samples (IC and DC) (Fig. 3B and C, respectively) the linear viscoelasticity range it extended up to 6 Pa, and thus stress of 5 Pa was selected for obtaining the spectrums of frequency sweep.

In the mechanical spectrum (Fig. 4) of non-cross-linked dispersions containing or not KT (Fig. 4A), in general, the samples exhibited predominantly elastic behavior with G′ values being approximately 2-fold higher than G″ values along the whole frequency range. However, the samples D15 and D15-KT showed predominantly viscous behavior, as their G″ values were higher than their G′ values along the whole frequency range (Table 3). Dynamic viscosity values of non-cross-linked samples does not presents no statistically significant differences between them (0–13.11) ($p<0.05$) (Table 3).

The highest G′ (393.5) and n′ (13.11) values were obtained for the sample D210-KT ($p<0.05$) (Table 3). Because of the increased polymer concentrations, a denser hydrogel structure is built in this sample. GG was previously reported to lead to denser structures by increased entanglement and packaging of double helices that reinforce the interchain interactions (Patil et al., 2012). On the other hand, according to Biliaderis (2009), after the retrogradation process, the starch favors the formation of a more organized and crystalline structure.

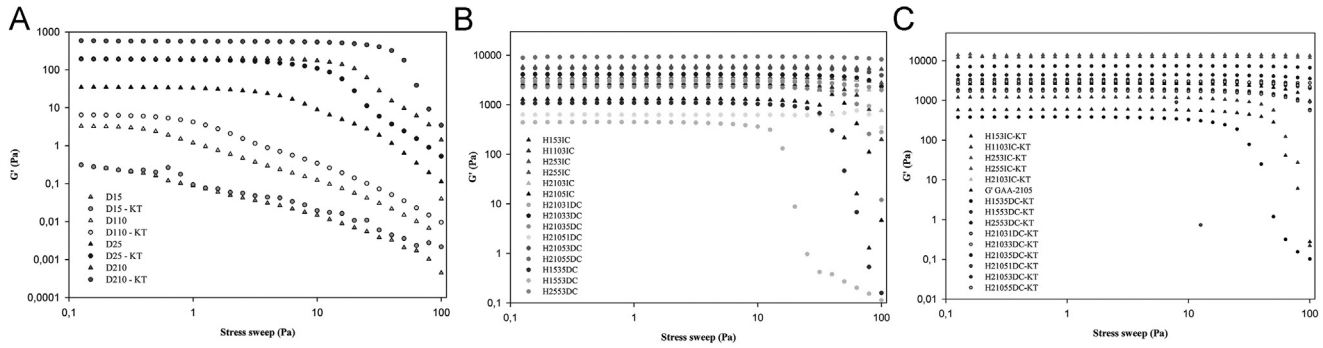

Fig. 3 – Stress (Pa) spectra of non-cross-linked dispersions containing or not KT (A), ionically and dually cross-linked GG/RS hydrogels without KT (B), ionically and dually cross-linked GG/RS containing KT (C).

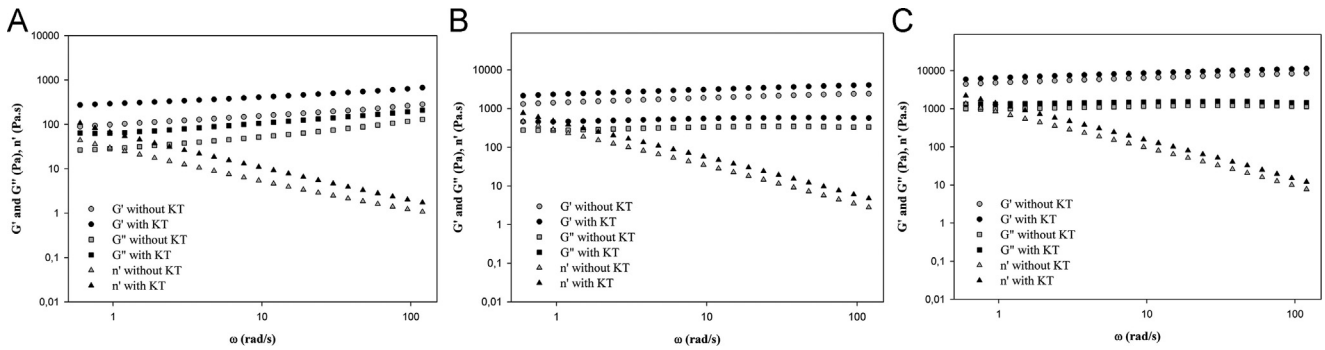

Fig. 4 – Mechanical spectra representative of (A) non-cross-linked GG/RS dispersions, (B) ionically and (C) dually cross-linked GG/RS hydrogels containing or not KT.

The ability of GG to form uniform networks with solid character at high concentration has previously been described in studies about viscoelastic and structural properties of unmodified starch/gellan blends. The contribution of starch to enhance the elasticity of the blends with other polymers was reported in studies with unmodified starch (Rodríguez-Hernández et al., 2006).

Besides, the KT should be entrapped in interstitial spaces of the polymeric chains, acting as physical cross-linking points in such structure, favoring the formation of a more packed and strength structure. Furthermore, the high concentration of cross-linker allows a higher cross-linking degree. This behavior evidenced that the blending and modification by cross-linking of these polymers promoted the formation of stronger structures.

Frequency sweeps of IC hydrogels with and without KT (Fig. 4B), demonstrated that the G′ values were approximately 5-fold higher than the G″ values along the whole frequency range (Table 3), revealing the predominantly elastic behavior of these samples. This can be attributed to the formation of a gel with a high cross-linking density (Carbinatto et al., 2012; Meneguin et al., 2014; Saxena et al., 2011; Soares et al., 2013).

In relation n′ values, among IC hydrogels there were no significant differences (1290.03–9159.33), but this values were higher than the non-cross-linked samples ($p<0.05$) (Table 3). The highest G′ values were obtained for hydrogels containing high polymers concentrations ($p<0.05$) (Table 3). In addition, G′ and G″ were parallel amongst themselves and independents of frequency. Such behaviors indicate that the ionic bonds between the cations and the double helices of both polymers promote the formation of strong and stable gels with an evident elastic character (Berger et al., 2004; Bigi et al., 2001; Kulkarni et al., 2011). It can be attributed to the high cross-linking degree of these samples, since the trivalent aluminum contributes to the formation of a strong and resistant gel. Each ion can establish three linkages with carboxylate groups of the hydroxyl groups of polymers, leading to stronger gel structure than those built with mono- or divalent cations (Maiti et al., 2011).

Khondkar et al. (2007) studied the rheological behavior of cross-linked starch and pectin gels with sodium trimetaphosphate and concluded that more resistant and elastic structures were reached after cross-linking.

In frequency sweep spectra of the DC hydrogels with or without KT (Fig. 4C), a predominantly elastic behavior was observed, since all spectra showed approximately 5-fold higher G′ values than G″ values along the whole frequency range. DC hydrogels containing higher polymer concentrations as well as the KT, presented increased G′ values, regardless of the concentration of Al^{3+} ($p<0.05$) (Table 3).

Moreover, G′ and G″ were parallel amongst themselves and frequency independent, indicating the formation of a strong gel (Carbinatto et al., 2012; Meneguin et al., 2014; Saxena et al., 2011; Soares et al., 2013). In general, it was observed larger n′ values for the samples containing the higher polymers concentrations, KT and Al^{3+}, regardless of the concentration of glutaraldehyde ($p < 0.05$) (Table 3).

Possibly, the structure assumes a new configuration with a high cross-linking degree when interchain covalent bonds were inserted in the polymer network, promoting strengthening and elasticity of the overall structure.

The role of glutaraldehyde in the strengthening of polymer structures and the improvement of elasticity was also observed in studies with gelatin films (Bigi et al., 2001).

For samples H21031DC, H21031DC-KT, H21033DC, H21033DC-KT, H21035DC, H21035DC-KT, H21051DC, and H21051DC-KT the G′ values overlapped across the frequency range, indicating that the incorporation of the KT did not significantly affect the rheological properties of these hydrogels ($p > 0.05$) as observed in the representative mechanical spectra (Fig. 4).

The results show that for IC and DC hydrogels, the highest G′ values were achieved when both polymers were in the maximum concentration and in the presence of KT ($p < 0.05$), leading to the formation of stronger structures. The highest n′ values was reached in the H21053DC-KT and H21055DC-KT samples (Table 3).

A quantitative analysis of the variation of G′ in function of the frequency was established from the linear regression analysis of G′ data in the mechanical spectra ($r^2 = 0.99$).

The linear regression values of the non-cross-linked were significantly lower (0.06–0.80) than those for the cross-linked hydrogels (0.83-0.99) ($p > 0.05$) (Table 3). These lower values are attributed to the formation of weaker structures, confirming the results observed in the mechanical spectra (Fig. 4). For IC and DC hydrogels, with and without KT, the *r* values were high (0.95–0.99 and 0.89–0.99, respectively) (Table 3), indicating the independence of frequency and also the formation of strong and stable gels after cross-linking (Carbinatto et al., 2012; Meneguin et al., 2014; Soares et al., 2013).

However, H153IC, H153IC-KT, H1535DC, H1535DC-KT, H1553DC, and H1553DC-KT presented the lowest *r* values (Table 3) and a higher dependence of frequency, which both are characteristic of weaker structures. The lower polymer concentrations present in these hydrogels should contribute to the formation of loose networks, due to the low level of entanglement and packing of the polymeric chains, as well as lower density of cross-linking under these conditions.

In a study with cross-linked hydrogels of agar and gelatin, Saxena et al. (2011) established a quantitative analysis of parameters (*S* and *n*) based on the "*Power Law*" (Eq. (1)) and these parameters was related to the cross-linking density and resistance of the hydrogels, as follows:

$$G' = S\omega^n \quad (1)$$

Where, G′ is the storage modulus, ω is the oscillatory frequency, *S* is the gel strength, and *n* is the viscoelastic exponent.

In an analysis similar to previously published reports (Meneguin et al., 2014; Saxena et al., 2011; Soares et al., 2013), the values of these parameters were determined by Eq. (1) (Table 3). Non-cross-linked dispersions, with or without KT, showed lower *S* values (0.00–244.19) and higher *n* values (0.22–55.17), confirming the formation of a weak structural network with low cross-linking density. These results are in agreement with the mechanical spectra (Fig. 4A) and with the linear regression results. For IC and DC hydrogels, in general, low *n* values and high *S* values were observed, confirming the formation of strong structures with a high cross-linking density (Table 3).

The *S* values for the IC (962.69–7171.01) and DC hydrogels (596.52–8592.95) (Table 3) were increased in the presence of drug and at high polymer concentration. This behavior can be attributed to the entrapment of drug particles in the interstitial space of the polymer network and an increased amount of polymers chains.

In the IC hydrogels, except for H2103IC-KT and H2105IC-KT, *S* values (Table 3) were low, indicating a low degree of cross-linking in relation to DC samples, consistent with the results presented in Fig. 4B. The decreased cross-linking density of such samples can result in weaker polymeric network and hydrogels that are less resistant to shear stress.

In DC hydrogels, the samples H21053DC-KT and H21055DC-KT with increased glutaraldehyde concentrations (3% and 5%) presented the highest *S* values (8592.95 and 8528.99, respectively) (Table 3), indicating the formation of tougher and more stable gels. This behavior can be attributed to the glutaraldehyde, which forms a highly interconnected structure, consolidated by intermolecular covalent linkages among the polymer chains. This is also confirmed by the results of the mechanical spectra for these samples (Fig. 4C).

The results showed that, in general, both cross-linking processes, IC and DC, as well as high polymer concentrations and the presence of the drug, favored the formation of stronger structures with predominantly elastic behavior, and that DC allowed the formation of more stable structures with the highest elasticity.

3.4. *Morphology of hydrogels*

Hydrogels selected by rheological assay (Table 4) were analyzed by FEG-SEM and photomicrographs of lyophilized non-cross-linked dispersions, IC and DC hydrogels, containing or not KT, were evaluate in order to verify the structural features.

Photomicrographs of the non-cross-linked dispersions (Fig. 5) reveled an irregular and dense structure, with some starch granules (Fig. 5E and F), indicating the formation of a more compact structure. This behavior can be related to the presence of RS-M2, whose structural network is more organized and packed with few porous, suggesting that the water is linked to starch chains becoming the structure more continuous (Yoon et al., 2009). Besides, the presence of GG in the system contributed to an increase of gel density. According to Rodríguez-Hernández et al. (2003) in studies about rheological properties of GG gels, the highest concentration of GG increased the interconnectivity of polymer chains, providing a higher level of structural organization. This behavior explains the higher density of D25 and D210 samples, containing or not KT (Fig. 5C–F), which containing high GG concentration, and corroborates with the data of rheological properties (Table 3), confirming the building of more compact structures on higher polymer concentrations.

In IC hydrogels (Fig. 6), in general, it was observed a more porous and irregular structural network compared to non-cross-linked dispersions (Fig. 5), mainly when KT was incorporated. However, in samples containing higher GG

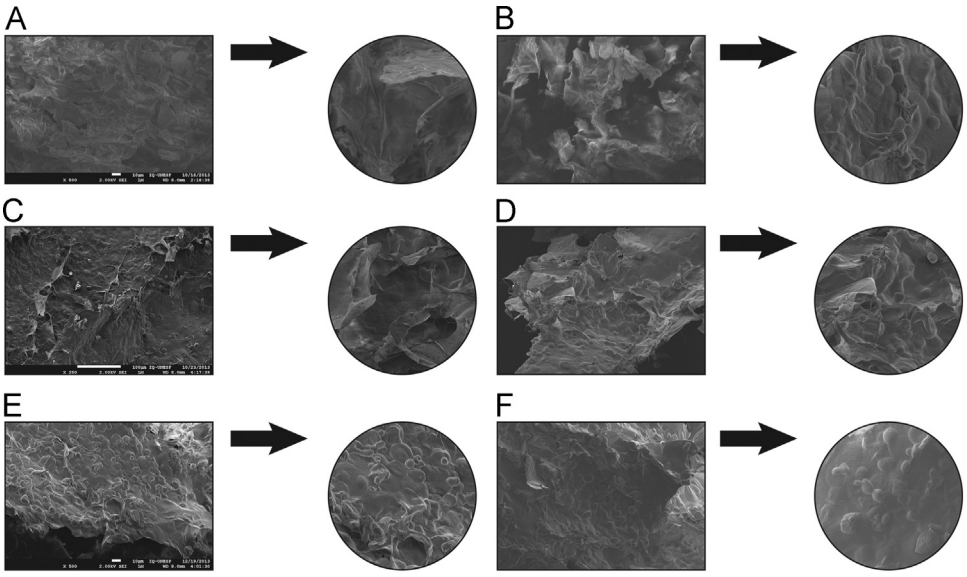

Fig. 5 – Scanning electron photomicrographs (SEM) of the non-cross-linked dispersions structures: (A) D15, (B) D15-KT; (C) D25, (D) D25-KT; (E) D210 and (F) D210-KT, with and without KT respectively, in increase 500 and 1000x.

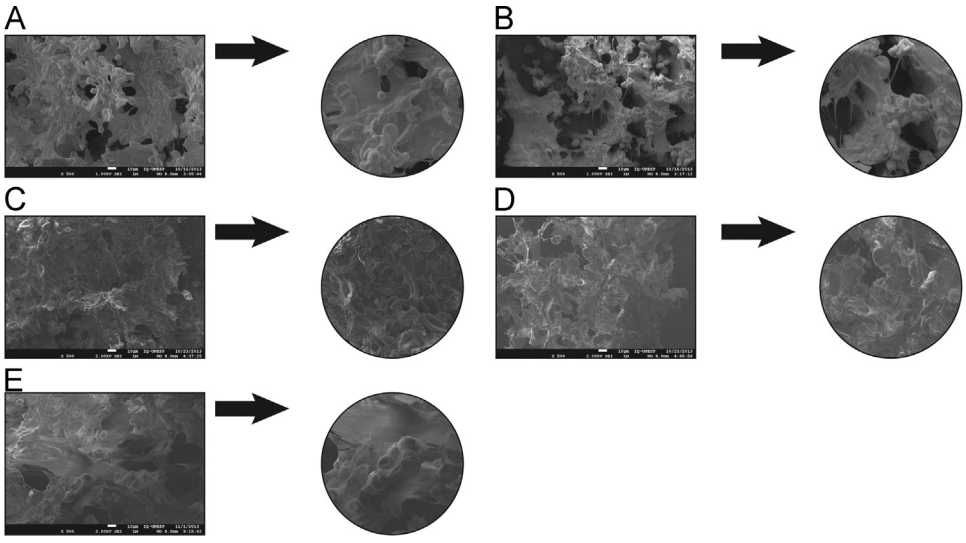

Fig. 6 – Scanning electron photomicrographs (SEM) of the ionically cross-linked hydrogels structures, (A) H153IC, (B) H153IC-KT; (C) H253IC, (D) H253IC-KT; (E) H255IC and (F) H255IC-KT, with and without KT respectively, in increase 500 and 1000x.

concentration (Fig. 6C–F), structural network was denser. This behavior can be attributed to the anionic character of GG that established possible strong interactions with the Al^{3+} ions. In this way, the molecules in dual helices aggregate, forming junctions zones that decrease the electrostatic repulsion between the chains, which become closer and originate a more packed network. Similarly behavior was reported by Maiti et al. (2011), in studies with GG microcapsules for the sustained release of glipizide.

The more porous structures built in the presence of KT (Fig. 6B, D and F) indicates that the drug was dispersed in the interstitial spaces among polymers chains acting as a plasticizer (Blasi et al., 2007; Ricci et al., 2005), resulting in a looser network.

In DC hydrogels (Fig. 7), denser network was observed, in relation to the IC hydrogels (Fig. 6). This feature must be due to the introduction of covalent bonds after cross-linking with glutaraldehyde, resulting in a tighter and inflexible structure with junctions more permanents and stable. This behavior corroborate the rheological analysis results, in which it was found that at DC hydrogels presented the highest values of S (Table 3), due to the high cross-linking degree.

The ability of glutaraldehyde to promote a strengthening at starch/gelatin blend microparticles was also reported by Phromsopha and Baimark (2014), who demonstrated that the cross-linking between the hydroxyl groups of polymer and the aldehyde groups of glutaraldehyde led to the formation a tridimensional structure with less mobile chains and more organized arrangements. Moreover, Berger et al. (2004) also observed that denser and packed networks can be achieved, more quickly, through ionic/covalent interactions.

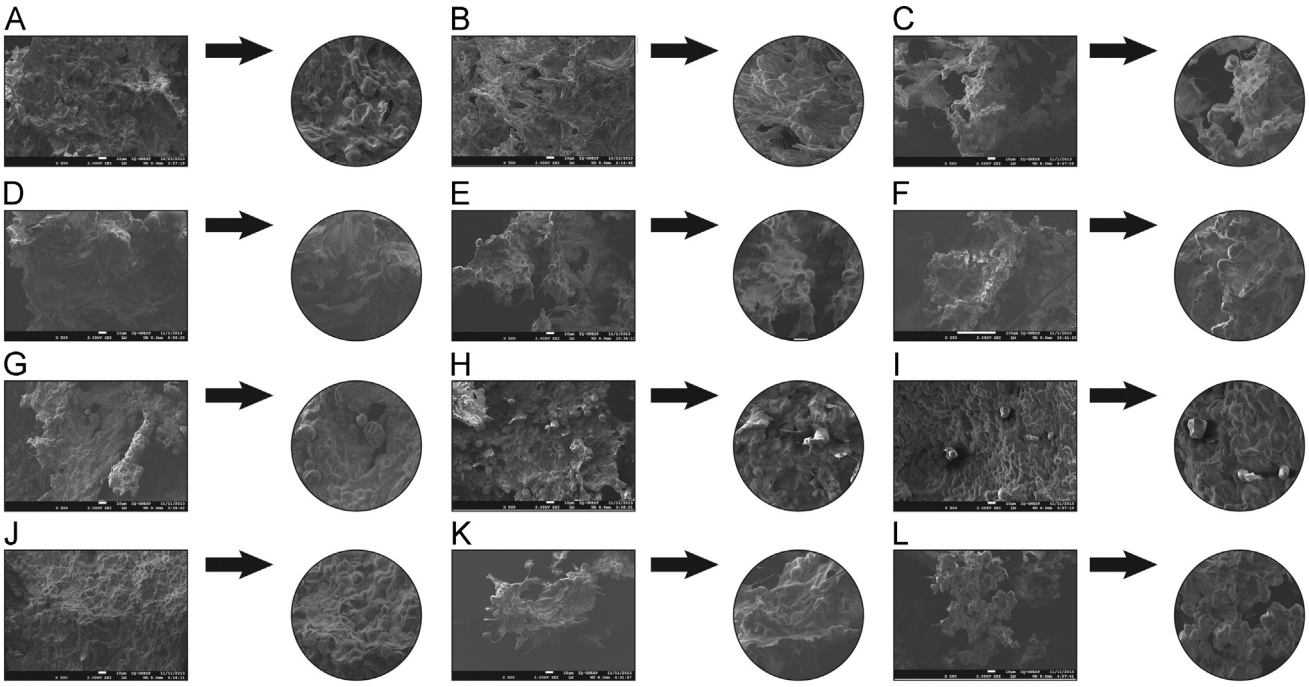

Fig. 7 – Scanning electron photomicrographs (SEM) of the dually cross-linked hydrogels structures: (A) H1535DC, (B) H1535DC-KT; (C) H2553DC, (D) H2553DC-KT; (E) H21031DC, (F) H21031DC-KT; (G) H21051DC, (H) H21051DC-KT; (I) H21053DC, (J) H21053DC-KT; (K) H21055DC and (L) H21055DC-KT, with and without KT respectively, in increase 500 and 1000x.

The highest polymer and cross-linkers concentrations contributed to formation of denser and continuous structures (Fig. 7D–M).

3.5. *X-ray diffraction (XRD) analysis*

In this work, the XRD studies were performed with the HAS, KT, GG, RS, non-cross-linked dispersions, IC and DC hydrogels.

Except for the drug, XRD patterns of all samples showed few peaks and a wide amorphous halo, indicating a typical behavior of semi-crystalline polymers with low crystallinity degree (Fig. 8). In fact, these polymers are not strictly amorphous, but the crystalline regions present in semi-crystalline polymers, many times, not exhibit X-rays scattering intensities sufficiently detectable (Mendes et al., 2016; Murthy and Minor, 1995).

The XRD pattern of KT (Fig. 8A) shows several intense and well defined peaks due the crystalline characteristics of this drug (Kim and Choi, 2002; Manna et al., 2007). Several peaks are displayed, mainly in low values of 2θ, at about 6.35° 14.4° 18.45° 22.9° 23.9° 27.65° and 29.5°, which is in agreement with the values reported by Yadav et al. (2013).

As HAS granules is a semi-crystalline material, it present three distinct polymorphous (A, B, and C) and varying crystallinity degree (Wang et al., 2015). The XRD pattern of HAS (Hylon VII®) (Fig. 8B) showed distinct amorphous halo and characteristic peaks indicating the semi-crystalline nature of this polymers. The peaks around 17°, 23° and 25° (2θ) are characteristic of the B-type polymorphous, while the peak in 19.8° is typical of V polymorph indicating a well-organized crystalline structure of amylose-lipid complexes present in the starch granules (Carbinatto et al., 2012; Freire et al., 2006; Shamai et al., 2003; Soares et al., 2013).

For GG was verified a diffraction pattern typical of semi-crystalline materials, characterized by a large amorphous halo with only two wider peaks, in around 9° and 20° (2θ) (Fig. 8C), similarly to those reported by Yang et al. (2013).

In the XRD pattern of RS (5% and 10%) (Figs. 8D and E, respectively), the peaks in approximately 17°, 23°, 25° (2θ) (B-type polymorphs) and 19.8° (2θ) (V- type polymorphs) were kept, but a significant reduction in intensity was observed. According to Mutungi et al. (2012), this behavior can be attributed to the presence of small-size crystallites that are embedded in a polymeric matrix and thus the x-rays scattering intensities are not sufficiently detected.

The peaks at 19.8° (2θ) were preserved in XRD pattern of retrograded starch (5% or 10%), indicating the V-type crystallinity which can be assigned complexation amylose-lipids (Karim et al., 2000; Liu et al., 2014; Shrestha et al., 2010; Zhou et al., 2014).

A new peak around 13° (2θ) (Figs. 8D and E) that also is typical of a V-type crystalline structure was observed. According Htoon et al. (2010), the starch retrogradation contributes to the change of the B-type polymorph for the V-type polymorph.

According to Cheetham and Tao (1998), starch containing a high amount of amylose (~65%) has low crystallinity (about 18%), attributed to the double helices packaging of amylopectin into clusters forming crystalline lamellae (Kibar et al., 2010). Despite the high amount of amylose present in material used in this study the XRD patterns showed that after hydrothermal treatment the structure was reordered.

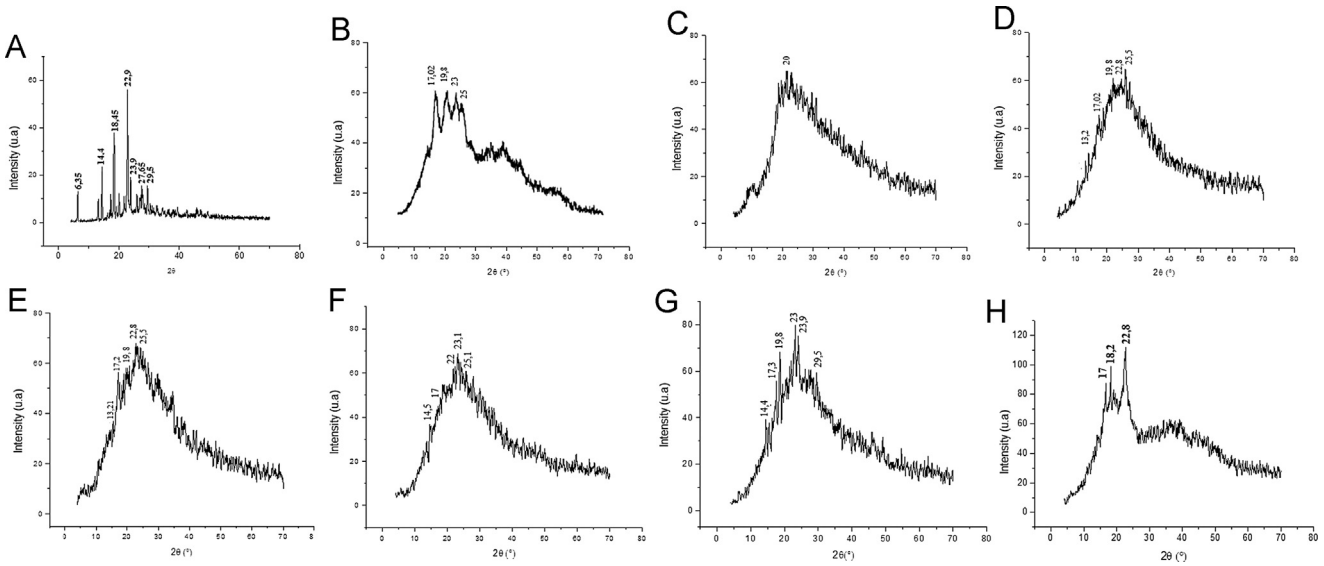

Fig. 8 – X-ray diffraction patterns of (A) KT, (B) high amylose (Hylon VII®), (C) gellan gum, (D) retrograded starch (5%) and (E) retrograded starch (10%), and representative X-ray diffraction patterns of (F) non-cross-linked GG/RS dispersions, (G) ionically and (I) dually cross-linked GG/RS hydrogels.

In XRD patterns of non-cross-linked dispersions, containing or not KT (Fig. 8F), the peaks of GG disappeared, possibly by overlapping of RS peaks present in the same regions. The characteristic peaks of the B-type polymorph at about 17°, 23° and 25° (2θ) were preserved in samples, but with lower intensity. The peaks about 19–19.8° (2θ) related to the presence of V-type crystalline structures of the amylose-lipid complexes were also preserved (Karim et al., 2000; Liu et al., 2014; Shrestha et al., 2010; Zhou et al., 2014). Besides, it was observed the appearance of a new peak at about 22° (2θ), characteristic of B-type crystalline structures (Liu et al., 2014; Zhou et al., 2014). Probably, after the combination of polymers, structural changes occur, resulting in the rearrangement of the polymer chains, so that structures with levels different of structural organization are built, resulting in different XRD patterns.

For non-cross-linked dispersions containing KT, the peak at 14.5° (2θ) (Fig. 8F) characteristic of the drug (Yadav et al., 2013) was maintained in all samples, while disappearance of some KT peaks may be attributed to overlapping with the more intense peaks of the RS in the same region, or by a dilution effect of the drug in the polymeric matrix.

The variation of the concentration of gellan did not affect significantly the XRD patterns, but the presence of peaks characteristics of the mixture of B- and V-type crystalline structures of RS was preserved.

In IC hydrogels, the GG characteristic peaks were not displayed (Fig. 8G) suggesting the GG dilution throughout the gel matrix or the overlapping with the stronger peaks of RS and/or KT at the same region.

The peaks related to B- and V-type polymorphs, characteristic of RS, also were preserved in IC samples, but with a reduced intensity, similarly to the RS patterns isolated (5% and 10%) (Figs. 8D and E). This low X-ray intensity again may be due to the small-size crystallites XRD pattern, that are embedded in polymeric matrix, reducing the diffraction effect.

In relation of KT, in general, its crystalline structure was preserved in all IC samples, evidenced by presence of well defined peaks around 14,4°, 18,4°, 23,9°, 27.6° and 29.5° (2θ) (Yadav et al., 2013), confirming that polymers blends and the obtaining process of hydrogels (ionic crosslinking) did not alter the drug crystalline structure. Besides, the RS patterns (B- and V-types polymorphs) were preserved in all samples and that the disappearance and/or appearance new peaks, can be attributed to alterations in the tridimensional network due to the cross-linking process, similarly to reported by Carbinatto et al. (2012), in studies with cross-linked pectin/HAS blends.

For DC hydrogels (Fig. 8H), without KT, in general, the GG peaks disappeared, due to a dilution effect or overlapping of its peaks by the RS peaks. The typical peaks of B- and V- type polymorphs were preserved, whereas in the H2553DC and H21055DC patterns, it was observed the appearance of a new peak at about 22° (2θ), related to B-type crystalline structure. The drug peaks about 18.4° and 22.9° (2θ) were preserved (Fig. 8H).

In general, the DC hydrogels XRD patterns displayed more intense peaks (Fig. 8H), indicating an increase of the crystallinity, in relation to the non-cross-linked and IC samples. This behavior can be attributed to the greater structural reorganization due to covalent bonds introduced by chemical cross-linking with glutaraldehyde, so that a more compact and stable structure was built. This finding corroborate the rheological data of DC hydrogels, which, in general, showed highest *S* values (Table 3), indicating the building of stronger and more resistant structure.

The data XRD analysis showed that the polymer semi-crystalline nature has been preserved, and that the high amount of crystallites present in RS matrix and crosslinking promoted important structural modifications. Besides, the higher polymers concentration and the DC contributed to the building of a more organized and stable structure. These results corroborate the rheological data, in which the DC

hydrogels exhibited predominantly more elastic behavior (strong response) in relation to IC hydrogels.

4. Conclusions

The retrogradation process promoted an improvement in the structural and textural properties of the starch. The retrogradation under cooling conditions (4 °C/8 days) contributed to the formation of a more organized and stable structural network, resulting in a more hard and cohesive material. On the other hand, the retrogradation in cycled temperature (4° and 30 °C/16 days) contributed to formation of a looser network with higher chains mobility, and demonstrated be more adhesive.

The blending of two natural polysaccharides (RS and GG), as well as their chemical modification, resulted in hydrogels with a wide range of mechanical and rheological properties, which can be modulated according to specific uses, by varying the polymer concentrations and altering the cross-linking process. Furthermore, the concentration of cross-linker can be modulated to optimize the texture property of the hydrogels.

The TPA data, in general, demonstrated that increased polymer concentrations enhanced the mechanical properties of hydrogels, including their hardness, adhesiveness, and cohesiveness. IC and the use of RS-M1 contributed to increased hardness and cohesiveness of the samples, while DC and RS-M2 increased adhesiveness. The rheological data demonstrated that for both cross-linking processes, the highest polymer concentrations and the presence of the drug, contribute to the formation of stronger and more stable structures with high elasticity. The DC process promoted the highest degree of cross-linking and elasticity of hydrogels. This behavior was confirmed by SEM images.

The data obtained from the XRD analysis revealed that the semi-crystalline nature of the polymers was preserved, and that the process of starch retrogradation and the chemical modification of the polymers by the IC and DC cross-linking promoted structural changes.

IC and DC processes were useful tools to modulate the mechanical properties of hydrogels in different ways so that, in general, the high polymers concentration and the presence of the drug favored the formation of predominantly elastic and stronger structures.

The higher values of G′, S and *n* of hydrogels H253IC-KT, H255IC-KT, H21053DC-KT and H21055DC-KT make them more promising materials because these features can be related with a higher stability of these systems in biological fluids, allowing a longer control of drug release rates. Besides, these hydrogels presented also good adhesiveness.

The mechanical and structural properties presented by these hydrogels make them promising materials for the design of new drug delivery systems that attend to different therapeutic needs.

Acknowledgments

Financial support was provided by CNPq (Conselho Nacional de Desenvolvimento Científico e Tecnológico) (Number Process 832236/1999-3) and CAPES (Coordenação de Aperfeiçoamento de Pessoal de Nível Superior).

REFERENCES

Agnihotri, S.A., Jawalkar, S.S., Aminabhavi, T.M., 2006. Controlled release of cephalexin through gellan gum beads: Effect of formulation parameters on entrapment efficiency, size, and drug release. Eur. J. Pharm. Biopharm. 63, 249–261.

Alvarez-Lorenzo, C., Blanco-Fernandez, B., Puga, A.M., Concheiro, A., 2013. Crosslinked ionic polysaccharides for stimuli-sensitive drug delivery. Adv. Drug Deliv. Rev. 65, 1148–1171.

Babu, R.J., Sathigari, S., Kumar, M.T., Pandit, J.K., 2010. Formulation of controlled release gellan gum macro beads of amoxicillin. Curr. Drug Deliv. 7, 36–43.

Bajpai, A.K., Shukla, S.K., Bhanu, S., Kankane, S., 2008. Responsive polymers in controlled drug delivery. Prog. Polym. Sci. 33, 1088–1118.

BeMiller, J.N., 2011. Pasting, paste, and gel properties of starch–hydrocolloid combinations. Carbohydr. Polym. 86, 386–423.

Berger, J., Reist, M., Mayer, J.M., Felt, O., Peppas, N.A., Gurny, R., 2004. Structure and interactions in covalently and ionically crosslinked chitosan hydrogels for biomedical applications. Eur. J. Pharm. Biopharm. 57, 19–34.

Bhardwaj, T.R., Kanwar, M., Lal, R., Gupta, A., 2000. Natural gums and modified natural gums as sustained-release carriers. Drug Dev. Ind. Pharm. 26, 1025–1038.

Bigi, A., Cojazzi, G., Panzavolta, S., Rubini, K., Roveri, N., 2001. Mechanical and thermal properties of gelatin films at different degrees of glutaraldehyde crosslinking. Biomaterials 22, 763–768.

Biliaderis, C.G., 2009. Chapter 8 - Structural Transitions and Related Physical Properties of Starch. In: BeMiller, J., Whistler, R. (Eds.), Starch Third Ed. Academic Press, San Diego, pp. 293–372.

Blasi, P., Schoubben, A., Giovagnoli, S., Perioli, L., Ricci, M., Rossi, C., 2007. Ketoprofen poly(lactide-co-glycolide) physical interaction. AAPS PharmSciTech 8, E78–E85.

Boni, F.I., Prezotti, F.G., Cury, B.S.F., 2015. Gellan gum microspheres crosslinked with trivalent ion: Effect of polymer and crosslinker concentrations on drug release and mucoadhesive properties. Drug Dev. Ind. Pharm., 1–29.

Calixto, G., Yoshii, A.C., Rocha e Silva, H., Stringhetti Ferreira Cury, B., Chorilli, M., 2015. Polyacrylic acid polymers hydrogels intended to topical drug delivery: preparation and characterization. Pharm. Dev. Technol. 20, 490–496.

Carbinatto, F.M., Castro, A.D., Cury, B.S.F., Magalhães, A., Evangelista, R.C., 2012. Physical properties of pectin–high amylose starch mixtures cross-linked with sodium trimetaphosphate. Int. J. Pharm. 423, 281–288.

Carbinatto, F.M., Castro, A.D., Evangelista, R.C., Cury, B.S.F., 2014. Insights into the swelling process and drug release mechanisms from cross-linked pectin/high amylose starch matrices. Asian J. Pharm. Sci. 9, 27–34.

Carvalho, F.C., Calixto, G., Hatakeyama, I.N., Luz, G.M., Gremião, M.P.D., Chorilli, M., 2013. Rheological, mechanical, and bioadhesive behavior of hydrogels to optimize skin delivery systems. Drug Dev. Ind. Pharm. 39, 1750–1757.

Chaturvedi, K., Ganguly, K., Nadagouda, M.N., Aminabhavi, T.M., 2013. Polymeric hydrogels for oral insulin delivery. J. Control. Release 165, 129–138.

Cheetham, N.W.H., Tao, L., 1998. Variation in crystalline type with amylose content in maize starch granules: an X-ray powder diffraction study. Carbohydr. Polym. 36, 277–284.
Chung, H.-J., Lim, H.S., Lim, S.-T., 2006. Effect of partial gelatinization and retrogradation on the enzymatic digestion of waxy rice starch. J. Cereal Sci. 43, 353–359.
Contri, R.V., Soares, R.M.D., Pohlmann, A.R., Guterres, S.S., 2014. Structural analysis of chitosan hydrogels containing polymeric nanocapsules. Mater. Sci. Eng.: C 42, 234–242.
Cury, B.S.F., Castro, A.D., Klein, S.I., Evangelista, R.C., 2009a. Influence of phosphated cross-linked high amylose on in vitro release of different drugs. Carbohydr. Polym. 78, 789–793.
Cury, B.S.F., Castro, A.D., Klein, S.I., Evangelista, R.C., 2009b. Modeling a system of phosphated cross-linked high amylose for controlled drug release. Part 2: physical parameters, cross-linking degrees and drug delivery relationships. Int. J. Pharm. 371, 8–15.
Denardin, C.C., Silva, L.Pd, 2009. Estrutura dos grânulos de amido e sua relação com propriedades físico-químicas. Ciênc. Rural 39, 945–954.
Dimantov, A., Greenberg, M., Kesselman, E., Shimoni, E., 2004a. Study of high amylose corn starch as food grade enteric coating in a microcapsule model system. Innov. Food Sci. Emerg. Technol. 5, 93–100.
Dimantov, A., Kesselman, E., Shimoni, E., 2004b. Surface characterization and dissolution properties of high amylose corn starch–pectin coatings. Food Hydrocoll. 18, 29–37.
Dinu, M., Schwarz, S., Dinu, I., Drăgan, E., 2012. Comparative rheological study of ionic semi-IPN composite hydrogels based on polyacrylamide and dextran sulphate and of polyacrylamide hydrogels. Colloid Polym. Sci. 290, 1647–1657.
Dona, A.C., Pages, G., Gilbert, R.G., Kuchel, P.W., 2010. Digestion of starch: in vivo and in vitro kinetic models used to characterise oligosaccharide or glucose release. Carbohydr. Polym. 80, 599–617.
Dragan, E.S., 2014. Design and applications of interpenetrating polymer network hydrogels. A review. Chem. Eng. J. 243, 572–590.
Freire, A.C., Podczeck, F., Sousa, J., Veiga, F., 2006. Liberação específica de fármacos para administração no cólon por via oral. I - O cólon como local de liberação de fármacos. Rev. Bras. De. Ciências Farm. 42, 319–335.
Gao, C., Ren, J., Zhao, C., Kong, W., Dai, Q., Chen, Q., Liu, C., Sun, R., 2016. Xylan-based temperature/pH sensitive hydrogels for drug controlled release. Carbohydr. Polym. 151, 189–197.
Giavasis, I., Harvey, L.M., McNeil, B., 2000. Gellan gum. Crit. Rev. Biotechnol. 20, 177–211.
Grassi, M.L., Grassi, R., Colombo, I, M., 2006. Rheology. In: Group, T.F. (Ed.), Understanding Drug Release and Absorption Mechanisms. CRC Press, New York, pp. 88.
Grattoni, C.A., Al-Sharji, H.H., Yang, C., Muggeridge, A.H., Zimmerman, R.W., 2001. Rheology and permeability of crosslinked polyacrylamide gel. J. Colloid Interface Sci. 240, 601–607.
Haralampu, S.G., 2000. Resistant starch – a review of the physical properties and biological impact of RS3. Carbohydr. Polym. 41, 285–292.
Hasheminya, S.-M., Dehghannya, J., 2013. An overview on production and applications of gellan biopolymer. Int. J. Agric. Crop Sci. 5, 3016.
Hennink, W.E., van Nostrum, C.F., 2012. Novel crosslinking methods to design hydrogels. Adv. Drug Deliv. Rev. 64 (Supplement), 223–236.
Hoffman, A.S., 2002. Hydrogels for biomedical applications. Adv. Drug Deliv. Rev. 54, 3–12.
Hou, H., Di Vona, M.L., Knauth, P., 2012. Building bridges: crosslinking of sulfonated aromatic polymers – A review. J. Membr. Sci. 423–424, 113–127.
Htoon, A., Shrestha, A.K., Flanagan, B.M., Lopez-Rubio, A., Bird, A. R., Gilbert, E.P., Gidley, M.J., 2009. Effects of processing high amylose maize starches under controlled conditions on structural organisation and amylase digestibility. Carbohydr. Polym. 75, 236–245.
Htoon, A.K., Uthayakumaran, S., Piyasiri, U., Appelqvist, I.A.M., López-Rubio, A., Gilbert, E.P., Mulder, R.J., 2010. The effect of acid dextrinisation on enzyme-resistant starch content in extruded maize starch. Food Chem. 120, 140–149.
Huang, M., Kennedy, J.F., Li, B., Xu, X., Xie, B.J., 2007. Characters of rice starch gel modified by gellan, carrageenan, and glucomannan: a texture profile analysis study. Carbohydr. Polym. 69, 411–418.
Jones, D., Woolfson, A.D., Brown, A., 1997. Textural analysis and flow rheometry of novel, bioadhesive antimicrobial oral gels. Pharm. Res 14, 450–457.
Karim, A.A., Norziah, M.H., Seow, C.C., 2000. Methods for the study of starch retrogradation. Food Chem. 71, 9–36.
Keawchaoon, L., Yoksan, R., 2011. Preparation, characterization and in vitro release study of carvacrol-loaded chitosan nanoparticles. Colloids Surf. B: Biointerfaces 84, 163–171.
Khondkar, D., Tester, R.F., Hudson, N., Karkalas, J., Morrow, J., 2007. Rheological behaviour of uncross-linked and cross-linked gelatinised waxy maize starch with pectin gels. Food Hydrocoll. 21, 1296–1301.
Kibar, E.A.A., Gönenç, I., Us, F., 2010. Gelatinization of waxy, normal and high amylose corn starches. GIDA - J. Food 35, 237–244.
Kim, J.-H., Choi, H.-K., 2002. Effect of additives on the crystallization and the permeation of ketoprofen from adhesive matrix. Int. J. Pharm. 236, 81–85.
Kulkarni, R.V., Mangond, B.S., Mutalik, S., Sa, B., 2011. Interpenetrating polymer network microcapsules of gellan gum and egg albumin entrapped with diltiazem–resin complex for controlled release application. Carbohydr. Polym. 83, 1001–1007.
Lau, M.H., Tang, J., Paulson, A.T., 2000. Texture profile and turbidity of gellan/gelatin mixed gels. Food Res. Int. 33, 665–671.
Lee, J.W., Park, J.H., Robinson, J.R., 2000. Bioadhesive-based dosage forms: the next generation. J. Pharm. Sci. 89, 850–866.
Li, W., Tian, X., Wang, P., Saleh, A.S.M., Luo, Q., Zheng, J., Ouyang, S., Zhang, G., 2016. Recrystallization characteristics of high hydrostatic pressure gelatinized normal and waxy corn starch. Int. J. Biol. Macromol. 83, 171–177.
Liu, H., Yu, L., Chen, L., Li, L., 2007. Retrogradation of corn starch after thermal treatment at different temperatures. Carbohydr. Polym. 69, 756–762.
Liu, L., Wang, D., Lian, X., Wu, H., 2014. Retrograded maize starch used as a medium to enrich Monascus from the air in winter. Int. J. Biol. Macromol. 67, 201–204.
Maiti, S., Ranjit, S., Mondol, R., Ray, S., Sa, B., 2011. Al+3 ion cross-linked and acetalated gellan hydrogel network beads for prolonged release of glipizide. Carbohydr. Polym. 85, 164–172.
Manna, L., Banchero, M., Sola, D., Ferri, A., Ronchetti, S., Sicardi, S., 2007. Impregnation of PVP microparticles with ketoprofen in the presence of supercritical CO2. J. Supercrit. Fluids 42, 378–384.
Martinez, A.W., Caves, J.M., Ravi, S., Li, W., Chaikof, E.L., 2014. Effects of crosslinking on the mechanical properties drug release, and cytocompatibility of protein polymers. Acta Biomater., 10.
Maulvi, F.A., Lakdawala, D.H., Shaikh, A.A., Desai, A.R., Choksi, H. H., Vaidya, R.J., Ranch, K.M., Koli, A.R., Vyas, B.A., Shah, D.O., 2016. In vitro and in vivo evaluation of novel implantation technology in hydrogel contact lenses for controlled drug delivery. J. Control. Release 226, 47–56.

Mendes, J.F., Paschoalin, R.T., Carmona, V.B., Sena Neto, A.R., Marques, A.C.P., Marconcini, J.M., Mattoso, L.H.C., Medeiros, E. S., Oliveira, J.E., 2016. Biodegradable polymer blends based on corn starch and thermoplastic chitosan processed by extrusion. Carbohydr. Polym. 137, 452–458.
Meneguin, A.B., Cury, B.S.F., Evangelista, R.C., 2014. Films from resistant starch-pectin dispersions intended for colonic drug delivery. Carbohydr. Polym. 99, 140–149.
Morris, E.R., Nishinari, K., Rinaudo, M., 2012. Gelation of gellan – A review. Food Hydrocoll. 28, 373–411.
Murthy, N.S., Minor, H., 1995. Analysis of poorly crystallized polymers using resolution enhanced X-ray diffraction scans. Polymer 36, 2499–2504.
Mutungi, C., Passauer, L., Onyango, C., Jaros, D., Rohm, H., 2012. Debranched cassava starch crystallinity determination by Raman spectroscopy: correlation of features in Raman spectra with X-ray diffraction and 13C CP/MAS NMR spectroscopy. Carbohydr. Polym. 87, 598–606.
Narkar, M., Sher, P., Pawar, A., 2010. Stomach-specific controlled release gellan beads of acid-soluble drug prepared by ionotropic gelation method. AAPS PharmSciTech 11, 267–277.
Ofokansi, K.C., Kenechukwu, F.C., Isah, A.B., Okigbo, E.L., 2013. Formulation and evaluation of elutaraldehyde-crosslinked chitosan microparticles for the delivery of ibuprofen. Trop. J. Pharm. Res. 12, 19–25.
Oliveira, G.F., Ferrari, P.C., Carvalho, L.Q., Evangelista, R.C., 2010. Chitosan–pectin multiparticulate systems associated with enteric polymers for colonic drug delivery. Carbohydr. Polym. 82, 1004–1009.
Paraginski, R.T., Vanier, N.L., Moomand, K., Oliveira, M., Zavareze, Ed.R., Silva, R.M., Ferreira, C.D., Elias, M.C., 2014. Characteristics of starch isolated from maize as a function of grain storage temperature. Carbohydr. Polym. 102, 88–94.
Park, E.Y., Baik, B.-K., Lim, S.-T., 2009. Influences of temperature-cycled storage on retrogradation and in vitro digestibility of waxy maize starch gel. J. Cereal Sci. 50, 43–48.
Patil, J., Kamalapur, M., Marapur, S., Kadam, D., 2010. Ionotropic gelation and polyelectrolyte complexation: the novel techniques to design hydrogel particulate sustained, modulated drug delivery system: a review. Dig. J. Nanomater. Biostruct. 5, 241–248.
Patil, P., Chavanke, D., Wagh, M., 2012. A review on ionotropic gelation method: novel approach for controlled gastroretentive gelispheres. International. J. Pharm. Pharm. Sci. 4, 27–32.
Patil, S., Sharma, S., Nimbalkar, A., Pawar, A., 2006. Study of formulation variables on properties of drug-gellan beads by factorial design. Drug Dev. Ind. Pharm. 32, 315–326.
Peppas, N.A., Bures, P., Leobandung, W., Ichikawa, H., 2000. Hydrogels in pharmaceutical formulations. Eur. J. Pharm. Biopharm. 50, 27–46.
Phromsopha, T., Baimark, Y., 2014. Preparation of starch/gelatin blend microparticles by a water-in-oil emulsion method for controlled release drug delivery. Int. J. Biomater. 2014, 6.
Prezotti, F.G., Cury, B.S.F., Evangelista, R.C., 2014. Mucoadhesive beads of gellan gum/pectin intended to controlled delivery of drugs. Carbohydr. Polym. 113, 286–295.
Prezotti, F.G., Meneguin, A.B., Evangelista, R.C., Cury, B.S.F., 2012. Preparation and characterization of free films of high amylose/pectin mixtures cross-linked with sodium trimetaphosphate. Drug Dev. Ind. Pharm. 38, 1354–1359.
Rajinikanth, P., Mishra, B., 2007. Preparation and in vitro characterization of gellan based floating beads of acetohydroxamic acid for eradication of H. pylori. Acta Pharm., 413.
Reddy, T., Tammishetti, S., 2002. Gastric resistant microbeads of metal ion cross-linked carboxymethyl guar gum for oral drug delivery. J. Microencapsul. 19, 311–318.
Ricci, M., Blasi, P., Giovagnoli, S., Rossi, C., Macchiarulo, G., Luca, G., Basta, G., Calafiore, R., 2005. Ketoprofen controlled release from composite microcapsules for cell encapsulation: effect on post-transplant acute inflammation. J. Control. Release 107, 395–407.
Rioux, B., Ispas-Szabo, P., Aït-Kadi, A., Mateescu, M.-A., Juhász, J., 2002. Structure-properties relationship in cross-linked high amylose starch cast films. Carbohydr. Polym. 50, 371–378.
Rodríguez-Hernández, A.I., Durand, S., Garnier, C., Tecante, A., Doublier, J.L., 2006. Rheology-structure properties of waxy maize starch–gellan mixtures. Food Hydrocoll. 20, 1223–1230.
Rodríguez-Hernández, A.I., Durand, S., Garnier, C., Tecante, A., Doublier, J.L., 2003. Rheology-structure properties of gellan systems: evidence of network formation at low gellan concentrations. Food Hydrocoll. 17, 621–628.
Romani, F., Corrieri, R., Braga, V., Ciardelli, F., 2002. Monitoring the chemical crosslinking of propylene polymers through rheology. Polymer 43, 1115–1131.
Salamat-Miller, N., Chittchang, M., Johnston, T.P., 2005. The use of mucoadhesive polymers in buccal drug delivery. Adv. Drug Deliv. Rev. 57, 1666–1691.
Saxena, A., Kaloti, M., Bohidar, H.B., 2011. Rheological properties of binary and ternary protein–polysaccharide co-hydrogels and comparative release kinetics of salbutamol sulphate from their matrices. Int. J. Biol. Macromol. 48, 263–270.
Shamai, K., Bianco-Peled, H., Shimoni, E., 2003. Polymorphism of resistant starch type III. Carbohydr. Polym. 54, 363–369.
Shrestha, A.K., Ng, C.S., Lopez-Rubio, A., Blazek, J., Gilbert, E.P., Gidley, M.J., 2010. Enzyme resistance and structural organization in extruded high amylose maize starch. Carbohydr. Polym. 80, 699–710.
Silverio, J., Fredriksson, H., Andersson, R., Eliasson, A.C., Åman, P., 2000. The effect of temperature cycling on the amylopectin retrogradation of starches with different amylopectin unit-chain length distribution. Carbohydr. Polym. 42, 175–184.
Singh, N., Singh, J., Kaur, L., Singh Sodhi, N., Singh Gill, B., 2003. Morphological, thermal and rheological properties of starches from different botanical sources. Food Chem. 81, 219–231.
Sinha, V.R., Kumria, R., 2001. Polysaccharides in colon-specific drug delivery. Int. J. Pharm. 224, 19–38.
Soares, G.A., Castro, A.Dd, Cury, B.S.F., Evangelista, R.C., 2013. Blends of cross-linked high amylose starch/pectin loaded with diclofenac. Carbohydr. Polym. 91, 135–142.
Souto-Maior, J.F.A., Reis, A.V., Pedreiro, L.N., Cavalcanti, O.A., 2010. Phosphated crosslinked pectin as a potential excipient for specific drug delivery: preparation and physicochemical characterization. Polym. Int. 59, 127–135.
Thompson, D.B., 2000. Strategies for the manufacture of resistant starch. Trends Food Sci. Technol. 11, 245–253.
Wang, S., Li, C., Copeland, L., Niu, Q., Wang, S., 2015. Starch retrogradation: a comprehensive review. Compr. Rev. Food Sci. Food Saf. 14, 568–585.
Yadav, P.S., Kumar, V., Singh, U.P., Bhat, H.R., Mazumder, B., 2013. Physicochemical characterization and in vitro dissolution studies of solid dispersions of ketoprofen with PVP K30 and d-mannitol. Saudi Pharm. J. 21, 77–84.
Yang, F., Xia, S., Tan, C., Zhang, X., 2013. Preparation and evaluation of chitosan-calcium-gellan gum beads for controlled release of protein. Eur. Food Res. Technol. 237, 467–479.
Yoon, H.S., Lee, J.H., Lim, S.T., 2009. Utilization of retrograded waxy maize starch gels as tablet matrix for controlled release of theophylline. Carbohydr. Polym. 76, 449–453.
Yu, S., Ma, Y., Sun, D.-W., 2009. Impact of amylose content on starch retrogradation and texture of cooked milled rice during storage. J. Cereal Sci. 50, 139–144.
Zavareze, Ed.R., Dias, A.R.G., 2011. Impact of heat-moisture treatment and annealing in starches: a review. Carbohydr. Polym. 83, 317–328.

Zhang, L., Hu, X., Xu, X., Jin, Z., Tian, Y., 2011. Slowly digestible starch prepared from rice starches by temperature-cycled retrogradation. Carbohydr. Polym. 84, 970–974.

Zhou, X., Baik, B.-K., Wang, R., Lim, S.-T., 2010. Retrogradation of waxy and normal corn starch gels by temperature cycling. J. Cereal Sci. 51, 57–65.

Zhou, Y., Meng, S., Chen, D., Zhu, X., Yuan, H., 2014. Structure characterization and hypoglycemic effects of dual modified resistant starch from indica rice starch. Carbohydr. Polym. 103, 81–86.